Mars Science Laboratory Launch-Arrival Space Study: A Pork Chop Plot Analysis

Alicia Dwyer Cianciolo[1,2], Richard Powell, Mary Kae Lockwood[3]
NASA Langley Research Center
MS 489
Hampton, VA 23681
757-864-8620
Alicia.M.DwyerCianciolo@nasa.gov

Abstract—Launch-Arrival, or "pork chop", plot analysis can provide mission designers with valuable information and insight into a specific launch and arrival space selected for a mission. The study begins with the array of entry states for each pair of selected Earth launch and Mars arrival dates, and nominal entry, descent and landing trajectories are simulated for each pair. Parameters of interest, such as maximum heat rate, are plotted in launch-arrival space. The plots help to quickly identify launch and arrival regions that are not feasible under current constraints or technology and also provide information as to what technologies may need to be developed to reach a desired region. This paper provides a discussion of the development, application, and results of a pork chop plot analysis to the Mars Science Laboratory mission. This technique is easily applicable to other missions at Mars and other destinations.

TABLE OF CONTENTS

1. INTRODUCTION

Past successful lander and rover missions to Mars have had landing ellipses on the order of 100's of km. The missions were limited to relatively low elevation (<-1 km) landing sites with minimal local hazards and the rovers have had limited range (10's of meters to a few kilometers). The Mars Science Laboratory (MSL) mission, scheduled for launch in 2009, will deliver an advanced rover to the surface Mars. MSL will allow for near global access to the planet (60 N to 60S, with elevations up to 2 km) and provide precision landing using guided entry (unlike Viking, Pathfinder, Mars Exploration Rovers (MER)) to land within 10 km of the target. The MSL lander is designed to have a nominal mission lifetime of approximately 3 Mars years and a rover range of 10 km. MSL technology will pave the way for Mars Sample Return Missions, potential Mars Scout missions as well as human exploration missions.

Unlike previous lander missions, the MSL entry heating environment differs due to turbulent transition before peak heating because of a combination of large vehicle size, high ballistic coefficient, and non-zero angle of attack. The results from 2001 MSL investigations showed that the turbulent heat flux would exceed stagnation point heating and will be a primary thermal protection system, TPS, design consideration. It is unclear if current flight qualified TPS technology is sufficient for the expected heating on MSL during entry or if technology advancement is required. In addition, it is unknown how the heating varies with the range of launch and arrival dates considered.

Based on the 2001 MSL heating investigation, indicators for leeside turbulent heating were developed. The heating indicators were provided by Karl Edquist of the MSL Aerothermal Working Group and were implemented into the Program to Optimize Simulated Trajectories II (POST2). Nominal entry trajectories for the pork chop study were simulated using POST2 for the range of launch and arrival dates. Arrival dates were constrained to Mars Solar Longitudes (L_s) between 70 to 210 deg (March 20, 2010 to February 13, 2011).[4] However, the remaining design space for MSL mission is quite broad: entry velocity could range from 5 to 7 km/s; type 1 and type 2 trajectories[5] are considered; additional level 1 requirements include a latitude range limited to +/-60 deg and a landing site elevation as high 2 km above the Mars Orbiter Laser Altimeter (MOLA) reference surface.

[1] U.S. Government work not protected by U.S. copyright.
[2] IEEEAC paper #1447, Version 4, Updated Dec. 8, 2005
[3] JHU/APL MS4-146 11100 Johns Hopkins Road Laurel, MD 20723

[4] Note that L_s is measured such that 0 deg denotes spring equinox, 90 deg denotes summer solstice, 180 deg autumnal equinox and 270 deg is winter solstice in the Northern Hemisphere.
[5] Type 1 trajectories travel 0 to 180 deg around the Sun before encountering Mars. Type 2 trajectories travel 180 to 360 deg around the Sun before encountering Mars.

The study presented herein investigates the variation in heating and other entry parameters (maximum deceleration, altitude at parachute deploy, time on parachute, etc) that result from changes in launch and arrival dates in order to determine available vehicle performance.

2. BACKGROUND

At the writing of this paper the MSL design was not in a final configuration. This study considers a 2003 MSL design, which includes a 2400 kg entry mass, 2 parachutes, a 4.572 m aeroshell, a skycrane terminal descent and 6 Viking derived descent engines. The MSL entry and decent are modeled using a high fidelity engineering end-to-end entry descent and landing (EDL) simulation built around NASA-Langley's Program to Optimize Simulated Trajectories II (POST2) [Ref 1, 2]. Details of the MSL entry, decent and landing are shown in Figure 1.

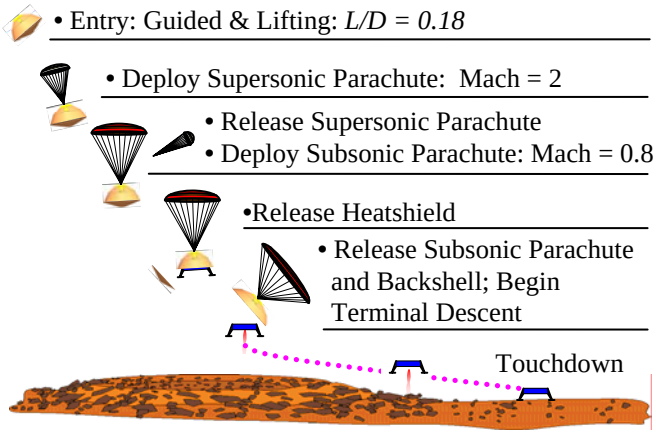

Figure 1. MSL Entry, Descent and Landing Sequence

The spacecraft is guided and navigated to a target entry corridor. Once the spacecraft encounters the Martian atmosphere, the entry guidance is activated. Bank angle commands are computed by the guidance system to direct the capsule's lift vector, shown in Figure 2, such that the desired position relative to the target landing site is achieved at the correct supersonic parachute deploy conditions. The bank angle magnitude is used to control the down range, and the bank angle direction is used to control cross range. Guided aeromaneuvering during entry is the technology that results in landing accuracies of less than +/- 10 km from the target.

Deployment of the supersonic parachute is triggered by the entry guidance logic to be within the Viking parachute qualification box of Mach 1.13 to Mach 2.2 and dynamic pressures of 239 to 850 Pa. The 16.15 m supersonic parachute is a derivative of the Viking mortar-deployed parachute and serves as a drogue parachute in this EDL system, decelerating the spacecraft to subsonic velocities. Once the vehicle reaches Mach 0.8, the backshell and supersonic parachute are jettisoned and a much larger, 32.7 m, subsonic main parachute is deployed to further slow the vehicle to a terminal velocity of 40 to 50 m/sec prior to initiation of powered decent. Once on the subsonic parachute, the heatshield is released.

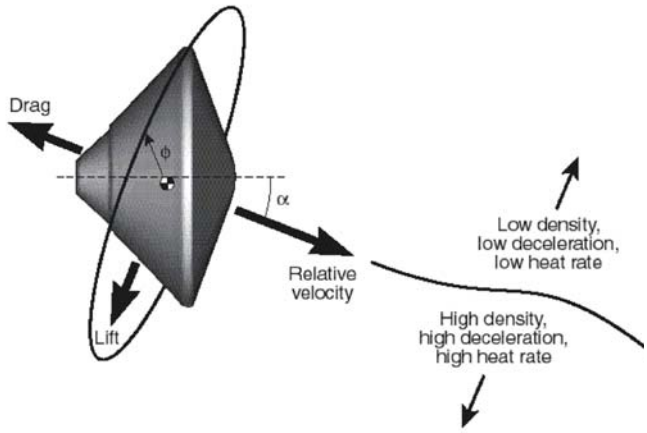

Figure 2. Hypersonic aeromaneuvering through bank angle modulation

During subsonic parachute decent, the radar is initiated, allowing the onboard navigation system to accurately determine the spacecraft's surface-relative altitude and velocity. At about 500 m above the surface the descent engines are ignited. Powered decent concludes with thrust termination approximately 1 m above the surface resulting in velocity components at touchdown well within the capabilities of the landing/arrest approaches under consideration. A skycrane phase in which the rover is lowered from the descent stage and then the descent stage flies away has been introduced into the mission baseline. However, the terminal descent portion of the MSL mission (from 1 km to the surface) is simplified to accommodate the large number (14,488 cases) of simulations required by the launch-arrival space. Details of the simplifications and modifications are discussed in detail later.

3. METHODOLOGY

A nominal POST2 simulation was developed to include the entry sequence described in the previous section. The study was performed for landing at the equator, 40 deg S and 60 deg S. The methodology described herein is similar for each latitude, however the discussion and results will focus on the equatorial site (0.33 deg S, 45.95 deg E).

Cartesian states for the MSL launch and arrival space were provided by Bill Strauss of the NASA Jet Propulsion Laboratory. The states included 157 launch dates and 176 arrival dates for a total of 27632 entry combinations. However, this analysis limited the max entry velocity allowable to 7 km/s, so only 14488 of the states were used for the study. All of the provided states had the same entry flight path angle, eFPA=-14.5 deg.[6] In order to perform parametric studies for characterization of the launch-arrival

[6] The FPA of –14.5 deg was the optimum for the guidance algorithm.

space analysis which required variations in eFPA, the Cartesian coordinates were converted to B-plane coordinates. For an illustration of the B-plane coordinate system, see Figure 3. The conversion from position and velocity to B-plane now enabled control of the B-plane angle, eFPA, velocity at infinity (Vinf) and the declination and right ascension of the Vinf vector. The simulation could now target altitude by controlling time on subsonic parachute, latitude could be targeted by controlling the B-plane angle and longitude by using a time offset to rotate the planet.[7]

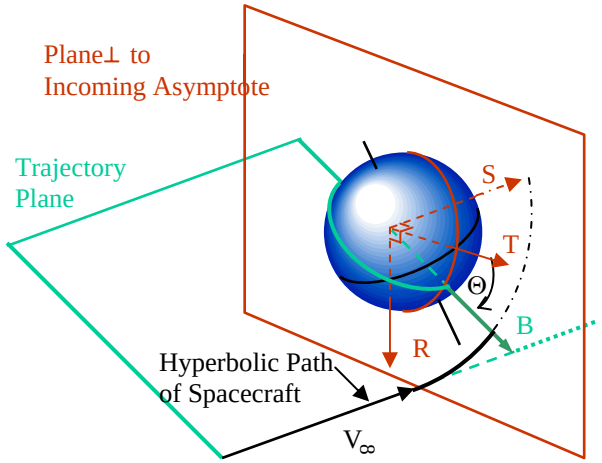

Figure 3. Illustration of the B-plane coordinate frame.[8]

Two parametric studies were required prior to running all 14488 initial states, also called pork chop cases. The first determined the time of day to enter and the second determined the entry flight path angle to be used for each case. What follows is a discussion of both studies.

Parametric Study #1: Determine Entry Local Time

Density in the atmosphere varies with time of day. The variations in density also affect the maximum heat rate, which is of concern for designing the TPS. The first parametric study identified the local true solar time (LTST) corresponding to the maximum heat rate. The heat rate is higher for higher entry velocities, therefore states at 7 km/s entry velocity were used. Figure 4 shows the variations in maximum heat rate using the current best estimate heating indicator [Ref 3] for a given range of eFPAs. For the equatorial site and eFPAs steeper than -12 deg, 10 a.m. resulted in the highest heat rate and this time was used when running the remaining 14488 cases.

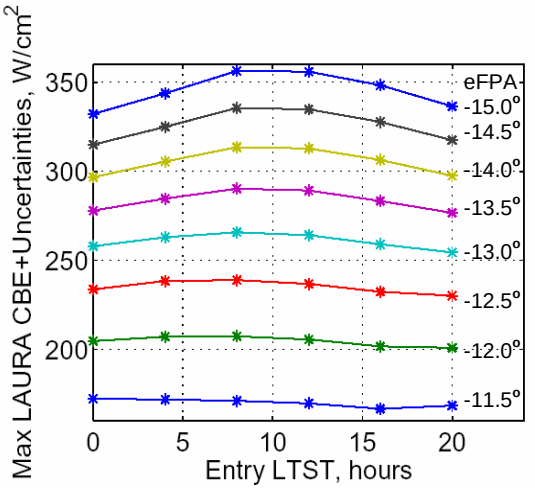

Figure 4. Heat rate vs. entry LTST for a range of entry flight path angles

Parametric Study #2: Determine Entry Flight Path Angle

After determining the entry LTST for all the cases, the second parametric study involved determining the eFPA for each case. It was noted that eFPA would depend on both entry velocity and L_s. The challenge was to accurately capture the dependence for all of the cases.

The criteria for determining an acceptable eFPA and time on parachute was based on previous MSL Monte Carlo analyses. To ensure safe landing, the vehicle must be on the subsonic parachute for a minimum of 70 seconds. Also to ensure an efficient entry, the trajectory was not allowed to loft. Lofting is defined as the point in the trajectory when the change in time of the radius vector to the vehicle becomes positive (rdot>0). The altitude versus velocity profile are shown for both a lofting (-12.0 deg; rdot = 38 m/s) and non-lofting (-14.5 deg; rdot = -36 m/s) trajectory in Figure 5. The sample trajectories with different eFPAs have entry velocities of 7 km/s at a L_s = 110 deg.

Figure 6 shows the time on chute (TOC) (left blue y-axis) and rdot (right green y-axis) over a range of eFPA which include the trajectories from Figure 5. The constraint lines for each parameter are included. Valid trajectories must fall between the two constraint lines. Notice that for an eFPA of -12 deg, neither the lofting nor the TOC constraints are met. An acceptable entry FPA for this L_s =110 and entry velocity = 7 km/s would have to be steeper (more negative) than -12.8 deg.

[7] Note that changing the time moves the location of the initial velocity vector, however, during the actual mission the targeting would be done prior to arrival at Mars.

[8] Where Θ is the B-plane angle, **S** is a unit vector in the direction of the incoming asymptote, **T** is a unit vector in the equator plane normal to **S**, **R** = **S** x **T** and B is the Impact Parameter.

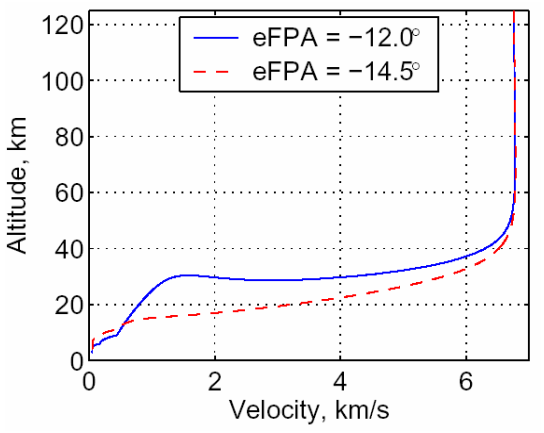

Figure 5. Altitude vs. velocity plot of lofting and non lofting trajectories

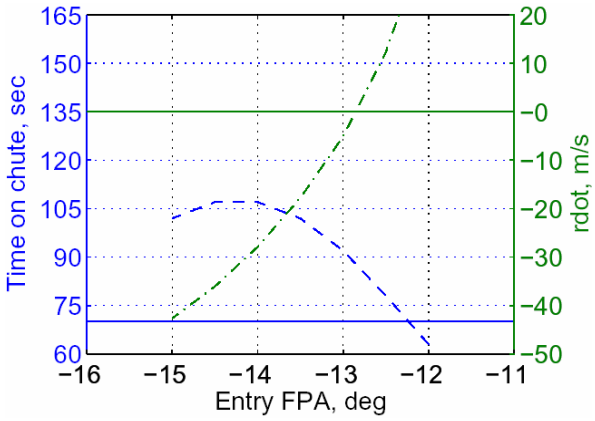

Figure 6. Time on chute and rdot versus entry flight path angle for the 7 km/s entry velocity and L_s = 110 deg

To determine the dependence on L_s, the L_s corresponding to the arrival dates for the 14488 pork chop cases are plotted versus entry velocity (see blue dots in Figure 7). Select values of L_s (see the red dots in Figure 7) were chosen at four entry velocities (5.5, 6.0, 6,5 and 7.0 km/s) with a range sufficient to capture the L_s distribution at the corresponding velocity. An eFPA sweep, or a nominal trajectory in which the eFPA varied from -11 to –15 deg in 0.5 deg increments, was run at each of the red dots using the 10 a.m. LTST discussed previously.

Figure 8 shows the eFPA sweep results of TOC and rdot for the L_s values circled in Figure 7. The top row of plots in Figure 8 are for L_s values = 110, 150 and 190 deg for 6.0 km/s entry velocity, the bottom row correspond to the same L_s values at 7.0 km/s entry velocity. Notice the value of the eFPA for rdot where it crosses the green rdot = 0 line (eFPA(rdot=0)). The eFPA(rdot=0) changes slightly but tends to increase (become less negative) as the L_s increases. Also the eFPA(rdot=0) value tends to get steeper as entry velocity increases thus establishing eFPA as a function of both L_s and entry velocity, (eFPA(L_s, entry velocity)). A similar trend does not hold for when the eFPA for TOC crosses the blue TOC = 70 sec line. But it is noted that in almost every case the eFPA(rdot=0 deg) is steeper than the eFPA(TOC =70 sec).

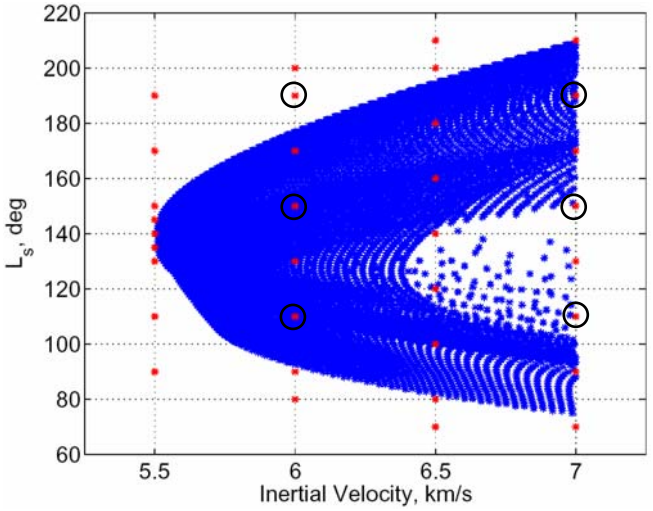

Figure 7. L_s vs. velocity for pork chop cases

Therefore, to insure that both the time on chute and lofting constraints were met in all cases, and to add margin into the eFPA calculation, the eFPA was selected to be eFPA(rdot =0) – 1 degree. For example, looking at the top left plot in Figure 8, L_s =110 for 6.0 km/s entry velocity case, the eFPA corresponding to rdot=0 is -12.6269 deg. Therefore, the eFPA used in the simulation table for L_s =110 deg, entry velocity = 6.0 km/s is –13.6269 deg. Table 1 contains the values used for the 6 km/s and 7 km/s entry velocity in the equatorial study based on Figure 8.

Table 1. Entry FPA (deg) as determined from Figure 7

Entry Velocity	6 km/s	7 km/s
L_s = 110 deg	-13.6269	-13.8539
L_s = 150 deg	-13.4736	-13.7517
L_s = 190 deg	-13.3122	-13.5760

Simulation Modifications

Several modifications were made to the simulation as mentioned in Section 2, “Background”, for purposes of simplicity and to decrease run time. Modifications were made to the entry guidance, subsonic parachute release logic and the terminal descent model. These modifications were based on analysis using the full MSL end-to-end EDL simulation.

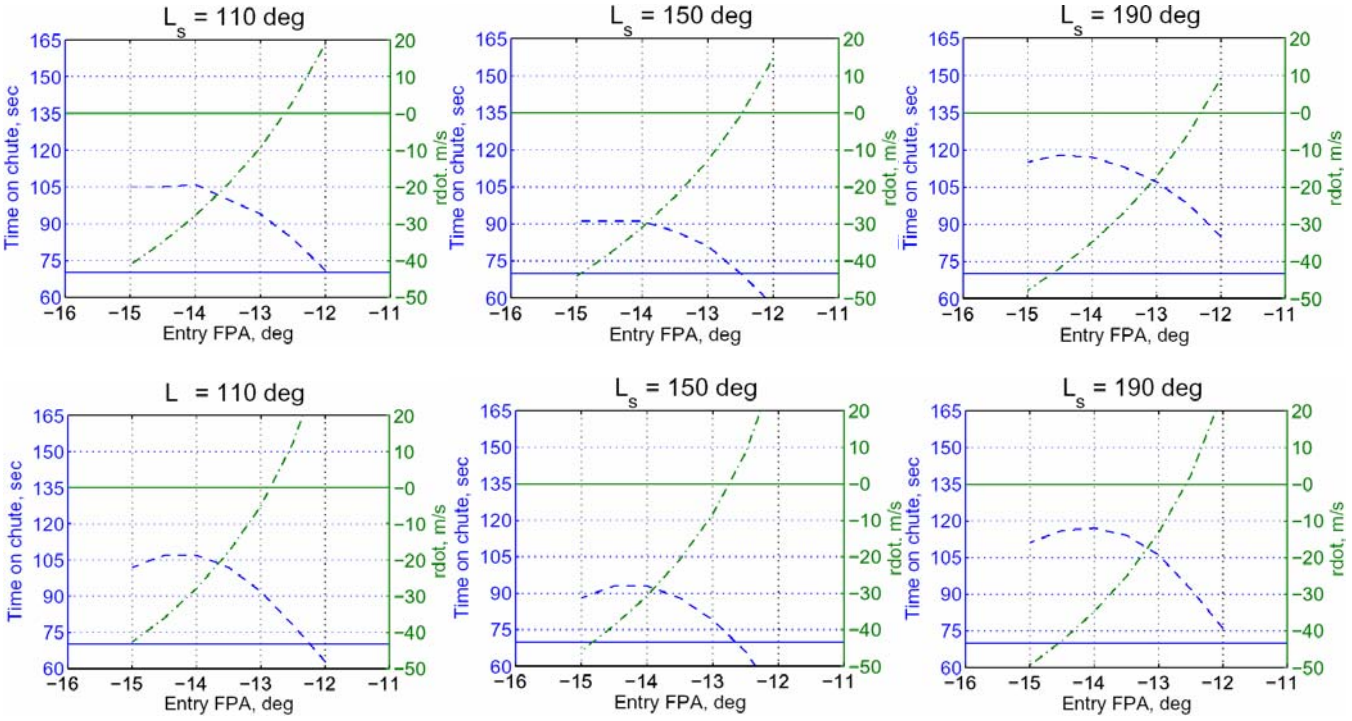

Figure 8. Results of the time on chute and rdot for entry flight path angle sweeps at various L_s values for 6 km/s entry velocity (top row) and 7 km/s (bottom row)

Gill Carman of the NASA Johnson Space Center (JSC) provided a bank angle profile for the 5.5 km/s and the 7 km/s entry velocity cases as a simplification to the original MSL entry guidance. A linear interpolation between the two tables was used to determine the bank profile for the remaining cases. The model neglects out of plane maneuvers. Figure 9 provides a plot of the bank profile for each reference entry velocity. The constant 20 deg bank angle at velocities less than 900 m/s approximated the heading alignment phase of flight.

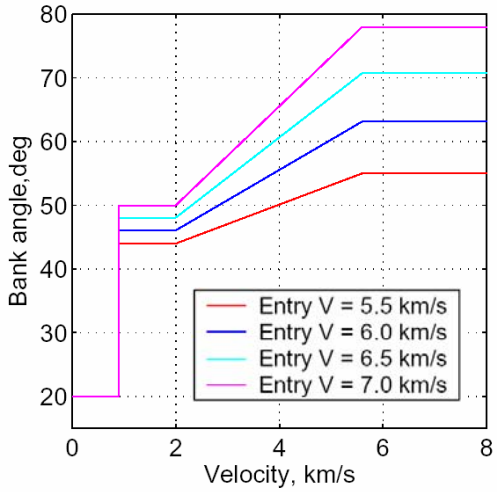

Figure 9. Bank profiles for reference entry velocities.

In the original MSL simulation, the terminal descent guidance is activated during the subsonic parachute phase. It operates in a surface fixed coordinate frame and solves a two point boundary value problem at each time step. As the vehicle descends on the parachute, the amount of initial thrust required to fly the thrust profile to steer the vehicle to a landing site (generally) increases. When required thrust (acceleration) reaches a threshold value, the parachute release is commanded and the engines are ignited. To save run time, a gravity turn was implemented, replacing the boundary value calculation. However, a method to model the parachute release was still needed.

Ron Sostaric of JSC used the guidance algorithm to calculate parachute release state for a series of reference cases employing a set of reasonable simplifying assumptions and provided a table of altitude versus velocity that represented parachute release conditions. The values are shown in Table 2.

Because of the large number of cases that needed to be run to complete the launch-arrival space study, each input was setup in such a way that minimized the possibility of the POST2 projected gradient optimizer to fail to target. This robustness was accomplished by using multiple problems in POST2 in which each problem was required to target only one variable using only one constraint. For example, each trajectory targeted the latitude, longitude and altitude of the landing site affected by B-plane angle, a time offset and time on the subsonic parachute respectively. So in problem one, the optimizer was only allowed to target latitude by optimizing B-plane angle. Once that problem was targeted it moved to the second problem were the optimizer was only allowed to target longitude by changing the time offset and holding the optimized value from the previous problem constant. This continued until an optimized value was obtained for each target parameter and a final problem ran all the optimized values to verify that the entire case was targeted.

4. RESULTS

Once the results of both the parametric studies and additional simplifying assumptions were incorporated into the POST2 simulation, each of the 14488 cases was run. The output parameters of primary concern for mission design are maximum heat rate, time on subsonic parachute, altitude at subsonic parachute deploy and maximum deceleration. The results are plotted in contours in launch and arrival space. In each of the pork chop plots, type one trajectories are shown in the right smaller lobe of the contours. Type 2 trajectories are on the left. A contour plot of inertial entry velocity is also included for reference and comparison.

To appreciate the information contained in pork chop plots, consider the heat rate contours shown in Figure 10. Using the current technology for MSL, the TPS has been qualified up to 210 W/cm^2. That would enable a launch and arrival space equal to the shaded area in Figure 10. At the equatorial site shown, comparing the location of the 210 W/cm^2 contour line in Figure 10 to the corresponding entry velocity contour line in Figure 11, the pork chop plot indicates that the mission would be limited to entry velocities less than 6.4 km/s. Therefore, the launch and arrival space is limited by the TPS constraint.

However, also consider, for example, that the Monte Carlo analysis at the equatorial site indicated that to ensure adequate timeline for the descent, the altitude of subsonic parachute deploy had to be greater than 5.6 km. Then the currently available shaded launch and arrival space in Figures 10 and 11 would be further reduced to meet the altitude of subsonic parachute deploy constraint. See Figure 12.

As mentioned earlier, previous Monte Carlo analysis indicated that 70 sec was the minimum time on the subsonic parachute to accomplish a successful descent. Figure 13 illustrates time on subsonic parachute displaying the minimum as 82 sec. Therefore, there is sufficient time on the parachute over the entire launch-arrival space considered and it does not further reduce the already constrained shaded area. As a final example, since this is not a human mission which would constrain the entry system to approximately 5g's, the max deceleration shown in Figure 14 also does not further constrain the shaded launch-arrival space.

Thus, for the simplified MSL example considered here, based only on a limited number of significant mission constraints (TPS, altitude at subsonic parachute deploy, time on parachute and max g's), the available launch space covers the entire window considered (July 30 to Dec. 27, 2009) but the arrival date is limited to July 7 to Oct. 16, 2010 for this equatorial site.

For simplicity and readability only single parameter contours are included in Figures 10 through 14. For design purposes, the plots can be overlaid, shaded, etc, until the available launch and arrival space can be outlined among all the constraints on a single plot. Only a few of the possible pork chop results are shown. In fact any output from POST2 can be considered in launch and arrival space. However the ones presented herein consist of some of the major parameters that influence the design of the mission. Pork chop plot analysis offers a quick method for mission designers to identify launch and arrival regions that are not accessible under current constraints or technology limitations. It also allows designers to determine what technologies need to be developed to reach a desired date.

5. CONCLUSIONS

Because the MSL mission is still broadly defined, with a large range of latitude, entry velocities, launch and arrival dates, time of day, and trajectory type yet to be selected, it is difficult to determine the design criteria for several mission parameters such as heat rate, or to answer questions about whether current technology can support the design space. Based on the results of this study, the launch and arrival space is constrained primarily by the heat rate constraint on the TPS, currently qualified to 210 W/cm^2. Additional constrains on the EDL system further reduce the accessible

Table 2. Subsonic parachute release logic

Vertical Velocity (m/s)	Subsonic Parachute Release Altitude (m)
40	275.5
45	338.5
50	421.7
55	506.1
60	590.9

launch-arrival space. The pork chop plot analysis described herein for the MSL mission was presented to the EDL mission design team. Based on the information, the team decided to limit the entry velocity of the MSL mission to 6 km/s. The pork chop technique provided mission designers with valuable information and insight into the specific launch and arrival space selected for the mission. The plots help to identify quickly launch and arrival regions that are not available under current constraints or technology and also provide information as to what technologies may need developed to reach a desired entry date.

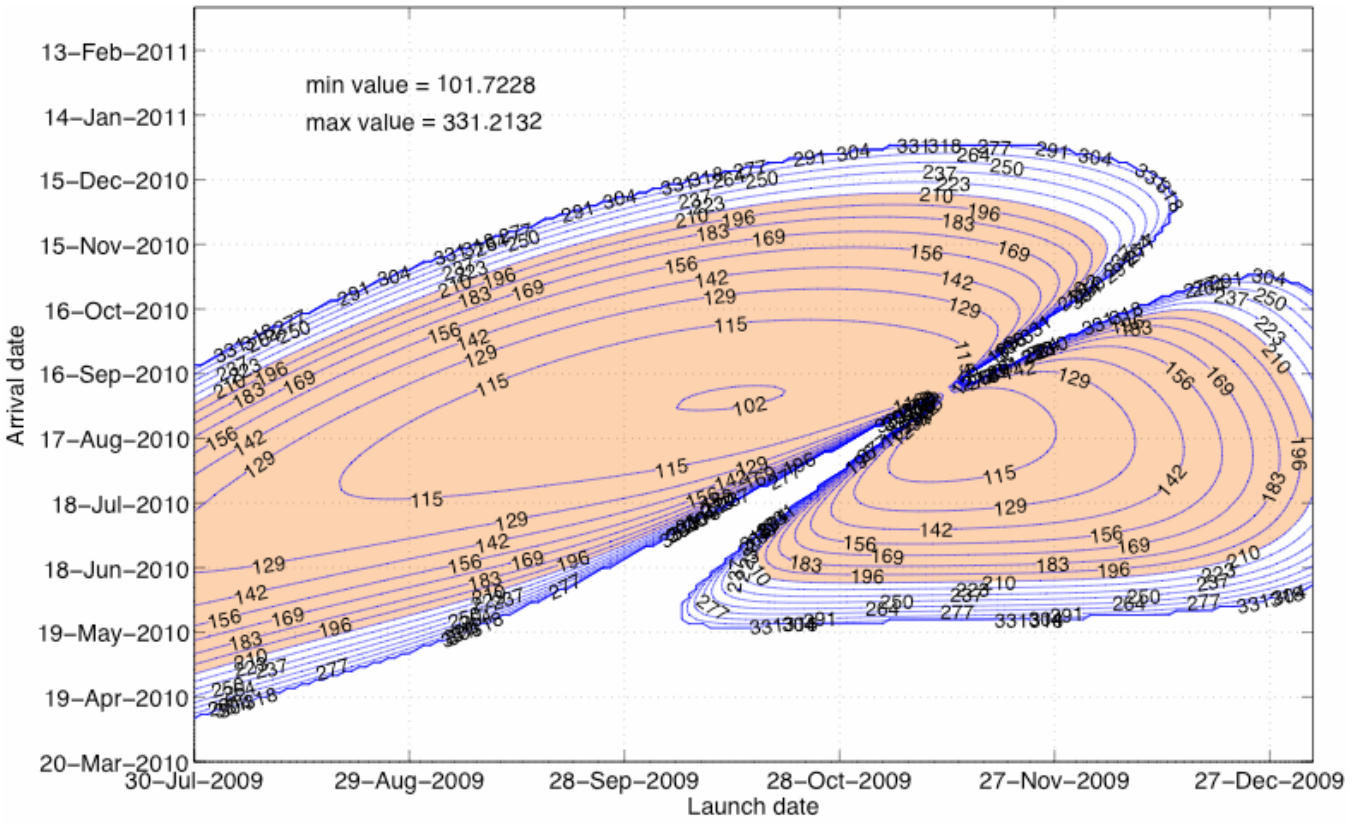

Figure 10. MSL max CBE LAURA + uncertainties aero heat rate indicator contours in launch and arrival space (W/cm^2)

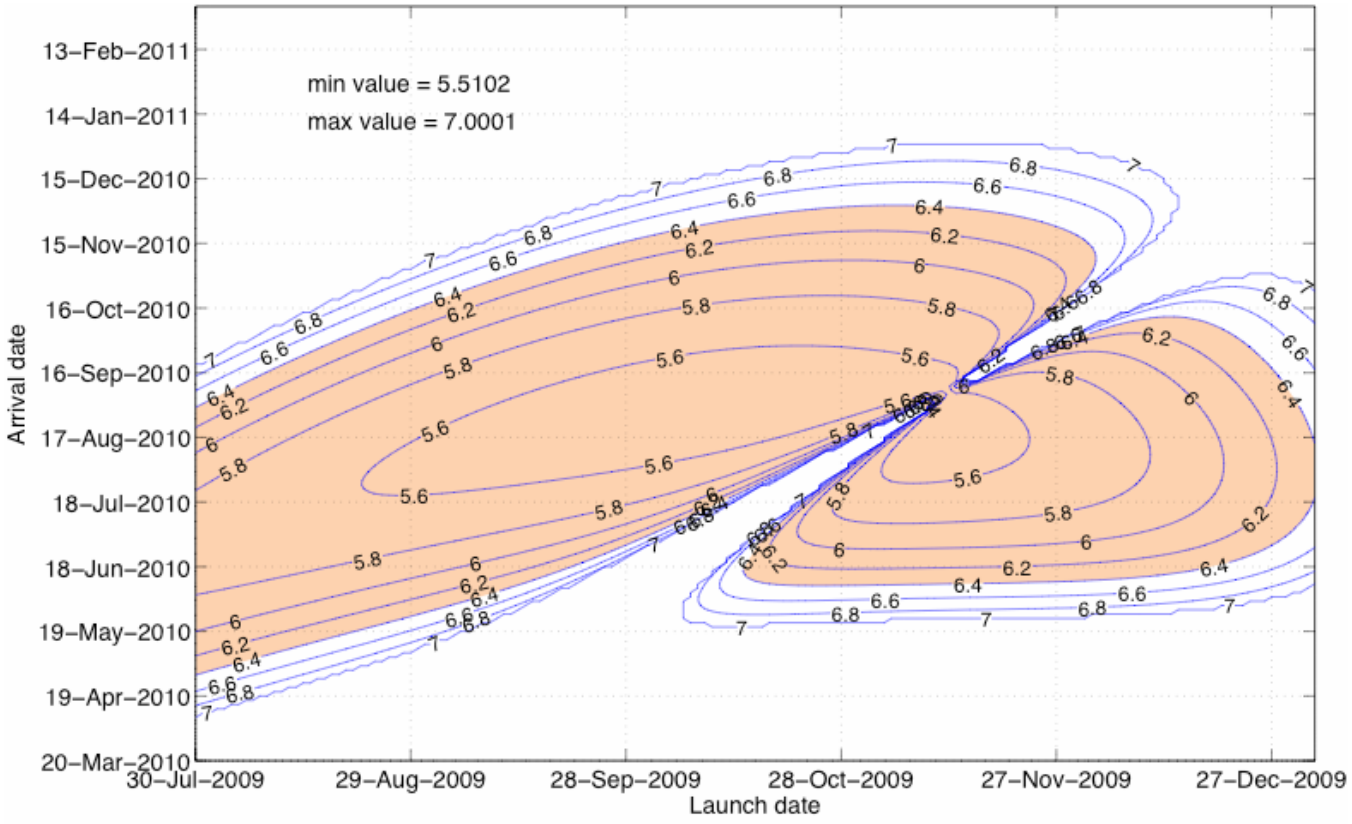

Figure 11. MSL entry velocity contours in launch and arrival space (km/s)

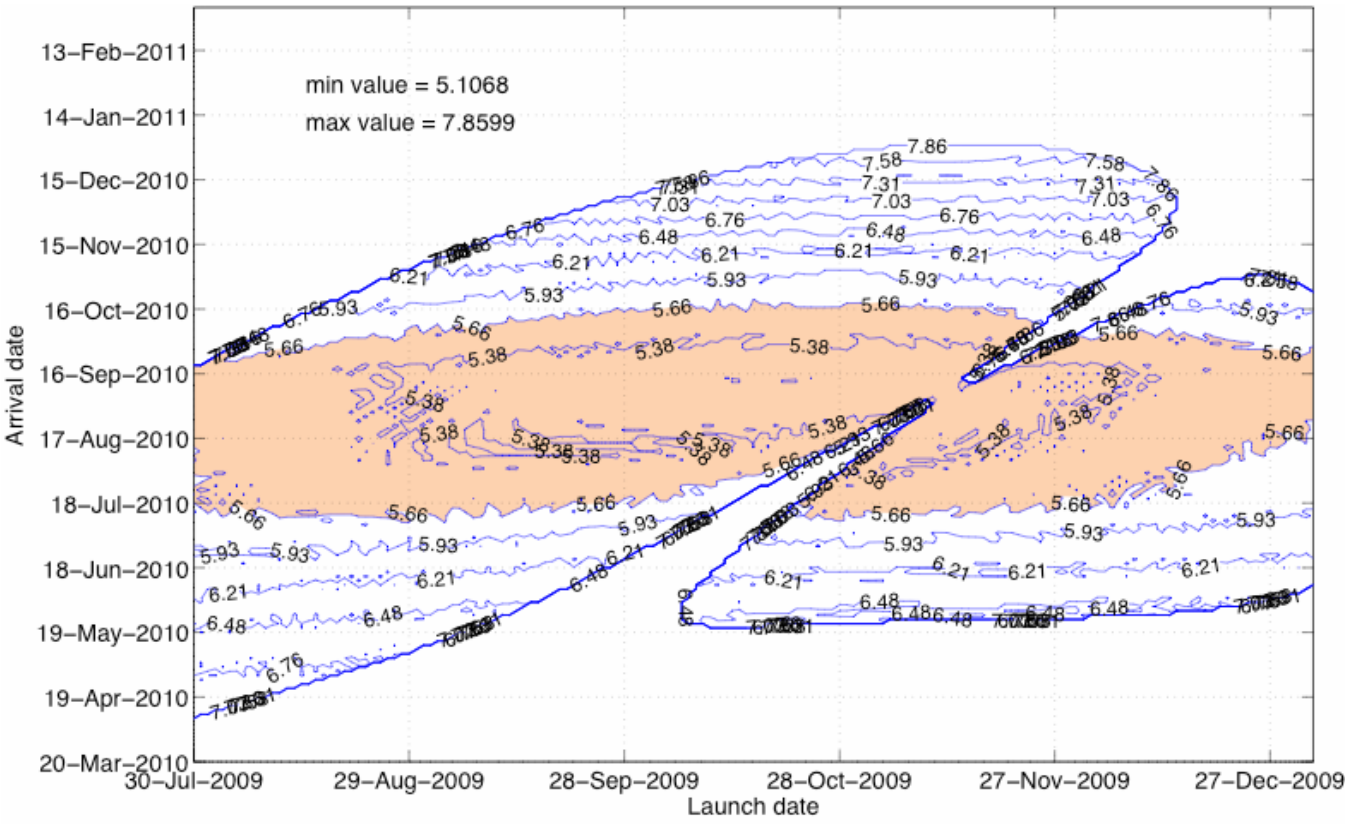

Figure 12. MSL altitude at subsonic parachute deploy contours in launch and arrival space (km)

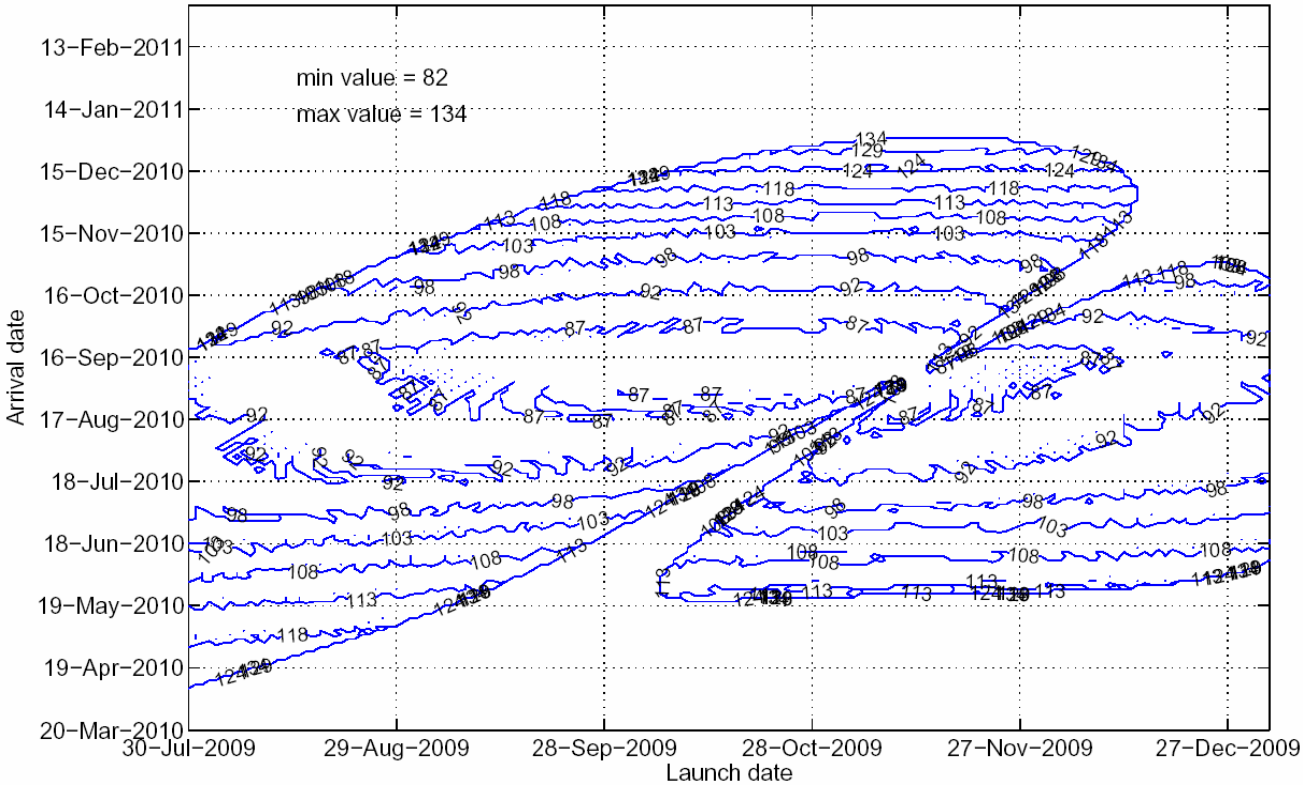

Figure 13. MSL time on subsonic parachute contours in launch and arrival space (sec)

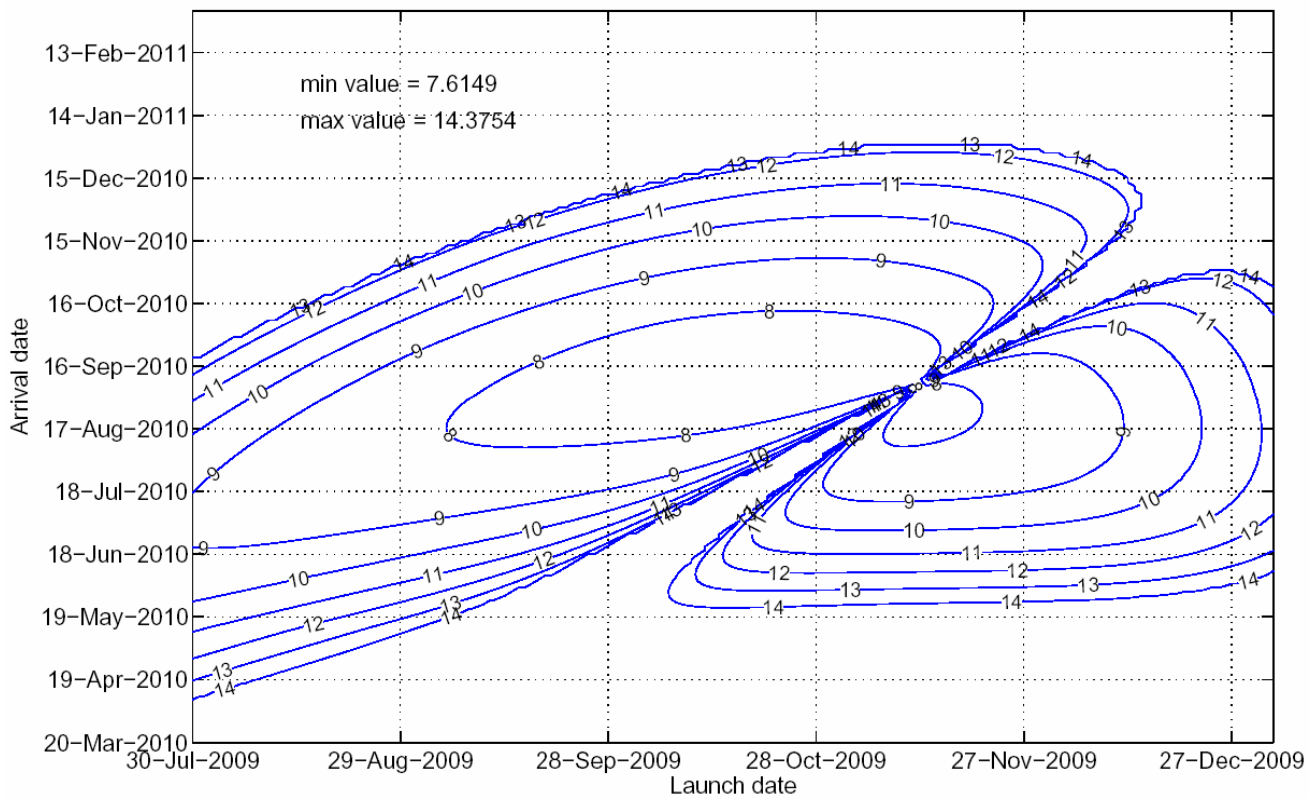

Figure 14. MSL max deceleration contours in launch and arrival space (g's: m/s^2)

However, even after an acceptable launch and arrival space have been identified, much more detailed analysis is required to finalize the design of the entry descent and landing. For example, an optimized closed loop entry guidance and entry flight path angle must be designed for the actual entry date; a local time, most likely different from the time corresponding to the max heat rate during the day will be used; and constraints on a lofting trajectory may be relaxed to optimize the final design.

ACKNOWLEDGEMENTS

The authors would like to acknowledge the following for their contributions: Bill Strauss, JPL, for providing entry states for each arrival latitude; Karl Edquist, LaRC, and the MSL Aerothermal Working group for providing heating indicators and assisting on the validation; Ron Sostaric, JSC, for providing parachute release model; and Gill Carman, JSC, for providing bank angle profiles for various velocities and masses.

REFERENCES

[1] Striepe, S. A., Way, D. W., Dwyer, A. M., and Balaram, J., "Mars Smart Lander Simulations for Entry, Descent, and Landing", AIAA Paper 2002-4412, Aug. 2002.

[2] Powell, R. W., Striepe, S. A., Desai, P. N., Queen, E. M., Tartabini, P. V., Brauer, G.L., Cornick, D. E., Olson, D. W., Petersen, F. M., Stevenson, R., Engle, M. C., Marsh, S. M., "Program to Optimize Simulated Trajectories (POST2), Vol. II Utilization Manual." Version 1.1.1G, May 2000, NASA Langley Research Center, Hampton VA.

[3] Olynik, D., et. al.: "New TPS Design Strategies for Planetary Entry Vehicle Design", AIAA Paper 1999-0348, 1999.

BIOGRAPHY

Alicia Dwyer Cianciolo is an aerospace engineer at the NASA Langley Research Center. Her work primarily focuses on the flight mechanics of missions, specifically the ascent and entry, descent and landing of various planetary missions. Her work has included flight operation for the Odyssey Aerobraking mission, and independent validation and verification for the EDL portion of the Mars Exploration Rovers. She has also been involved with work on the Mars Reconnaissance Orbiter and Mars Sample Return mission as well as Scout proposals and advanced studies for defining technology requirements for next generation missions to Mars. She has a bachelor's degree in physics from Creighton University and a master's degree in mechanical engineering from The George Washington University.